

## **Interactions of relativistic particles in stellar winds**

Santiago del Palacio,<sup>1</sup> Gustavo E. Romero,<sup>1</sup> and Valentí Bosch-Ramon<sup>2</sup>

<sup>1</sup>*Facultad de Ciencias Astronómicas y Geofísicas de La Plata, Universidad Nacional de La Plata, Argentina.*

<sup>2</sup>*Facultat de Física, Universitat de Barcelona, España.*

**Abstract.** Several binary systems hosting a massive star and a companion that is either a similar star or a compact object, present non-thermal emission from radio to  $\gamma$ -rays. This non-thermal emission is the consequence of the interactions of relativistic particles surrounded by the stellar wind. The main goal of this work is to characterize the high-energy physics of  $\gamma$ -ray binaries by implementing a general modeling for their most important high-energy processes. To thoroughly investigate the effects of the emitter-star-observer geometry on the resulting radiation, we systematically applied a non-thermal leptonic model for different locations of the emitter, magnetic fields, and acceleration timescales. The results of this procedure are presented in the form of emissivity maps, which are useful for exploring statistical properties of  $\gamma$ -ray binaries as well as their expected distribution in the galaxy.

### **1. Introduction**

Some of the most luminous galactic sources are high-mass binary systems in which one of the components is a massive star of spectral type OB. This type of binaries present non-thermal emission in the radio and X-ray bands, which suggests the presence of a population of relativistic charged particles (e.g. Mirabel & Rodríguez 1994, Barret 2004). Also, some of these systems have been detected in high energies (HE;  $E > 100$  MeV) and/or very high energies (VHE;  $E > 100$  GeV) (Dubus 2013, Paredes et al 2013), which shows that they can be efficient accelerators and  $\gamma$ -ray emitters.

Depending on the nature of the companion (Cn), the systems can be classified as a microquasar, a binary hosting a young pulsar, or a massive star binary. In a microquasar, the Cn is a stellar-mass black hole (BH), or a neutron star (NS) with a weak magnetic field, capable of accreting material coming from the star and generating relativistic jets (Mirabel & Rodríguez 1999); in a binary with pulsar, the Cn is a young NS with a strong magnetic field that powers an intense relativistic wind (Maraschi & Treves 1981); finally, in a massive star binary the Cn is another massive star with a strong stellar wind (e.g. Eichler & Usov 1993, Benaglia & Romero 2003). Note that the high-energy phenomena is similar in all these systems, which in many cases leads to uncertainties in determining the nature of the Cn.

The non-thermal emission from high-mass binaries is generated by ultra-relativistic particles accelerated, generally, in strong shock-waves in plasma flows. The non-thermal energy could be supplied by accretion and transported by jets in microquasars, or carried by supersonic winds of massive stars or the relativistic wind of a pulsar. Most of the accelerated particles cool down locally through interactions with the medium matter,

magnetic and radiation fields. The result at high energies of these interactions depends strongly on the massive star, as it provides targets (mostly ultraviolet photons) for Inverse Compton (IC) scattering, and target atomic nuclei for proton-proton interactions and relativistic Bremsstrahlung, among other radiation processes. Under general conditions within gamma-ray binaries (i.e., magnetic field strengths of the order of 1 G and photon field energy densities of the order of  $1 \text{ erg/cm}^3$ ), however, leptons cool down and radiate more efficiently than hadrons. Additionally, the radiation coming from the inner regions of a high-mass binary is likely to undergo absorption due to pair creation in the stellar radiation field (for an assessment of the importance of the different processes, see Bosch-Ramon & Khangulyan 2009).

In this work, we take advantage of the few assumptions required by a simple model, which can be useful to sketch in a generic way the physical properties of these objects. Considering the present and future observational developments, which imply an increase in the quantity of known sources, we apply this model to investigate in detail the physical processes that underlie their high-energy emission.

The structure of this article is as follows: in Section 2, we present the most important aspects of the one-zone model; in Section 3, we apply this tool for different choices of the relevant state parameters; and finally, in Section 4, we discuss our results in the context of the current observational data, and summarize the main conclusions of this work.

## 2. Model

From a generic point of view, high-mass binary systems can be characterized by the presence of a massive star and an accelerator of relativistic particles. We consider both the massive star and the accelerator as point-like objects, and thus homogeneous. In addition, the accelerator and the emitter are assumed steady and co-spatial, as electrons cannot travel long distances while emitting because of the short cooling timescales. This is known as a *one-zone model*, which is the simplest model capable of incorporating the most relevant physical processes of a given system, and of reproducing the main features of its observable quantities.

The injection of relativistic electrons in the emitter is taken to follow an energy distribution  $Q(E) \propto E^{-2} \exp(-E/E_{\text{max}})$  for energies above 1 GeV up to few  $E_{\text{max}}$  (the cutoff energy), consistent with a Fermi I acceleration process. The restriction of our analysis to particles with energy above 1 GeV is in order to concentrate on the emission above GeV energies; moreover, the most energetic particles cool down faster and therefore locally, which allows us to neglect the non-radiative losses (i.e., particle escape and adiabatic cooling). Particle maximum energy ( $E_{\text{max}}$ ) is obtained by equating their cooling time (taking into account synchrotron and IC losses) to their acceleration time, plus the constraint derived from comparing the accelerator/emitter size ( $R$ ) and the particle gyroradius:  $R > r_g = E_{\text{max}}/qB$ . To minimize the number of free parameters, we assumed the characteristic acceleration time to be  $t_{\text{acc}} = E/(\eta Bc q)$ , where  $E$ ,  $q$  and  $c$  are the particle energy, charge and velocity, respectively; the parameter  $\eta$  is the acceleration efficiency, which we assume to be constant. Note that  $\eta$  is limited to the range  $(0, 1)$ , with  $\eta = 1$  being the maximum efficiency, which corresponds to assuming Bohm diffusion in the acceleration process.

The relativistic electrons interact with the ambient stellar photon field and with the emitter magnetic field, producing a broad radiation spectrum. The dominant ra-

diative processes are IC scattering and synchrotron, whereas the dominant VHE  $\gamma$ -ray absorption process is pair production with stellar photons (Gould & Schreder 1967). We have not considered radiation reprocessing, although for weak enough magnetic fields an electromagnetic IC cascade can develop, increasing the transparency to VHE photons, and for stronger fields, the secondary pair radiation can overcome the X-rays from the primary electron distribution in the emitter (e.g. Bosch-Ramon et al. 2008). We have also assumed that the emitting flow is at most mildly relativistic, as it would be the case for a standing shock in a jet or a wind-colliding region, and thus we have not accounted for Doppler boosting, which would increase the model geometrical parameters. Finally, we assumed a distance to the source of  $d = 3$  kpc, and a characteristic scale of  $a = 3 \times 10^{12}$  cm related to the size of the binary system; for the companion star, we adopted a luminosity of  $L_* = 3 \times 10^{38}$  erg/s and an effective temperature of  $T_* = 3 \times 10^4$  K; for the accelerator, we assumed an injection luminosity of  $L_{\text{inj}} = 10^{36}$  erg/s (for comparative purposes, the estimated values of these parameters for the system LS 5039 are  $d = 2.9$  kpc,  $T_* = 3.9 \times 10^4$  K,  $L_* = 7 \times 10^{38}$  erg/s,  $a = 2.3 \times 10^{12}$  cm, and  $L_{\text{inj}} < 10^{37}$  erg/s, while for the system PSR B1259-63 they are  $d = 2.3$  kpc,  $T_* = 3.4 \times 10^4$  K,  $L_* = 3.7 \times 10^{38}$  erg/s,  $a = 1.2 \times 10^{14}$  cm,  $L_{\text{inj}} < 8 \times 10^{35}$  erg/s). As a result, only two free parameters are left in our model: the acceleration efficiency  $\eta$ , and the ratio of the magnetic field energy density to the radiation field energy density,  $\delta = u_{\text{mag}}/u_{\text{rad}}$ . Once these parameters are given certain values, the steady-state electron energy distribution can be computed (see e.g. Khangulyan et al. 2007).

### 3. Results

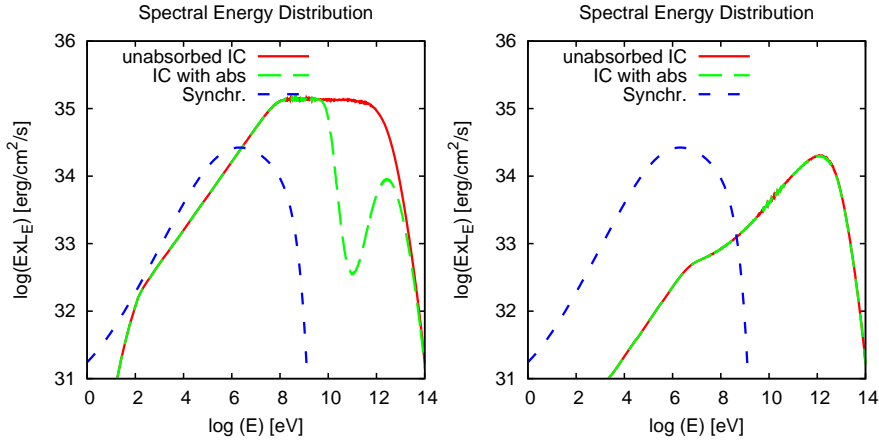


Figure 1. SEDs for a weak magnetic field ( $\delta = 10^{-4}$ ) and a high acceleration efficiency ( $\eta = 1$ ). The left figure was calculated for an emitter behind the star, located at  $(-2a, a)$ , while the right one was calculated for an emitter in front of the star, located at  $(2a, a)$ . In both cases the observer is in the direction of the positive  $x$ -axis and the massive star is at  $(0, 0)$ .

The spectral energy distribution (SED) is a measure of the amount of energy emitted per time and area units in a certain frequency (or energy). Because the radiative and absorption processes have a strong dependence with the interaction angle, the star-

emitter-observer geometry plays a crucial role in the resulting HE and VHE spectrum. In order to investigate this factor we calculated the SED for different positions of the emitter with respect to the massive star and the observer. In Fig. 1 we present the SEDs for two different positions of the emitter in a case dominated by the radiation field ( $\delta = 10^{-4}$ ) and a highly efficient accelerator ( $\eta = 1$ ). The HE radiation produced by IC scattering in the observer direction is greater if the emitter is behind the massive star; however, the  $\gamma$ -ray absorption is also enhanced in this configuration, resulting in a diminished VHE flux.

To study the geometrical aspects in which we are interested, and considering that the emitter structure and location within the system is not known, it is useful to display in maps relevant features of the emitter for all the possible locations. To do so, we compute the particle population and the (absorbed) emission from an emitter placed at a specific position in the star-emitter-observer plane, and then we extract any relevant quantity for such a location. This procedure is repeated for every spatial coordinate in the star-emitter-observer plane, and the result is displayed in the form of a two-dimensional map. These maps are studied in the context of physical constraints (related to energy requirements and confinement of the emitter), empirical constraints (scenarios that yield a very intense emission are considered unlikely as there are very few known systems with such characteristics) and instrumental constraints (energy fluxes below the sensitivity of the present instruments cannot be detected).

We focus here on the total energy flux in the ranges: 0.3–10 keV ( $F_X$ ), 0.1–10 GeV ( $F_{\text{GeV}}$ ) and 0.1–10 TeV ( $F_{\text{TeV}}$ ). Furthermore, to probe the validity of the point-like emitter assumption, we estimate the minimum emitter radius considering balance between the ram pressure of the stellar wind and the non-thermal electron pressure, which gives a lower limit for the emitter pressure. We normalize this value to the stellar distance ( $r$ ), and consider the approximation to remain valid as long as  $R/r < 0.5$ . For illustrative purposes, emissivity maps for a specific case are shown in Fig. 2.

#### 4. Discussion

We explored in detail the radiation coming from systems of orbital separation  $a > 3 \times 10^{12}$  cm with a *one-zone* leptonic model. This model works well for sources with  $L_{\text{inj}} < 10^{36}$  erg/s, and it reflects the relevant features of the emission and absorption processes, mainly the geometry role in the detectability of  $\gamma$ -rays. However, the validity of the approximation is dubious for sources with a high acceleration efficiency, a low magnetic field, and an emitter located at  $r > 6a$ , as in those regions the value of  $R/r$  is highest, with  $R/r \sim 0.5$  in such cases.

Some conclusions of our results are:

- In general, sources with low magnetic fields have a higher TeV luminosity, unless the sources host very inefficient accelerators that can hardly reach TeV energies.
- Sources with strong magnetic fields have a higher X-ray luminosity, and in most cases the predicted X-ray luminosity is far above the instrumental sensitivity threshold, which suggests that such sources could be detected even at distances larger than 3 kpc.
- There must be very few powerful sources with a high acceleration efficiency and a weak magnetic field at a distance  $\sim 3$  kpc, as otherwise it would overpredict the

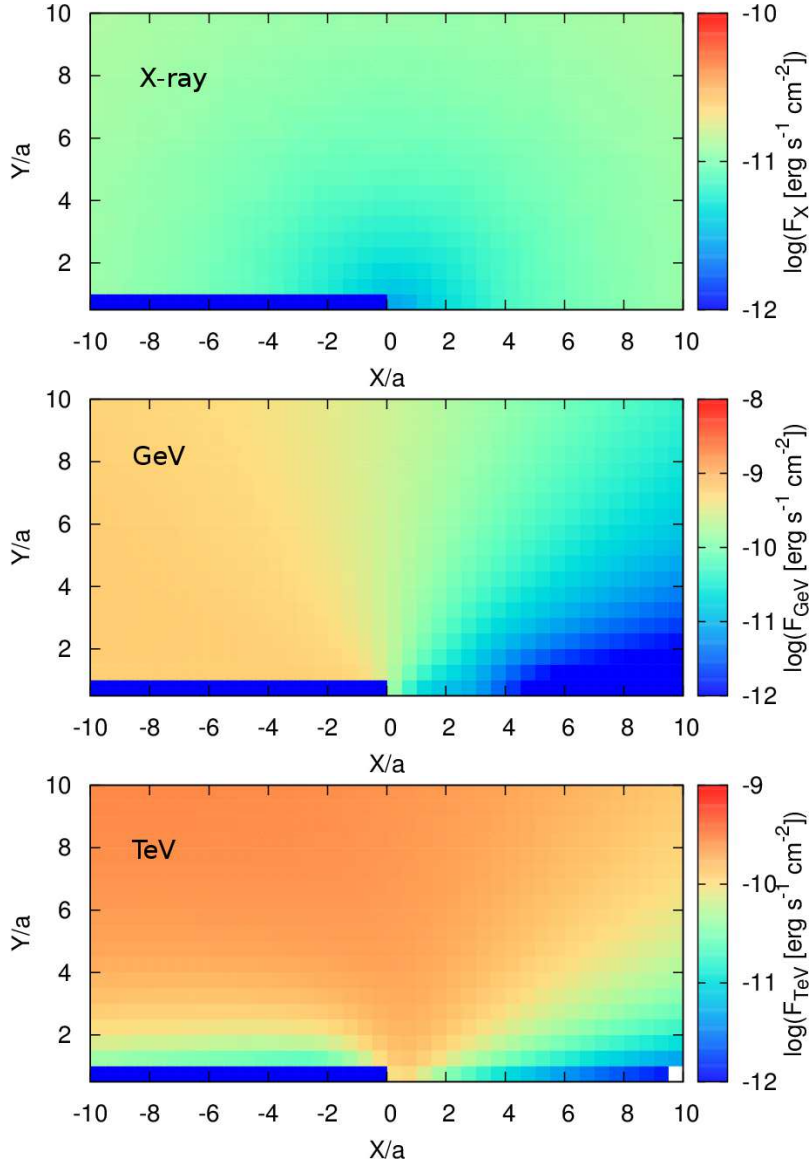


Figure 2. Emission maps in the X-ray, GeV, and TeV bands (top left, top right, and bottom left panels, respectively) for a weak magnetic field ( $\delta = 10^{-4}$ ) and a high acceleration efficiency ( $\eta = 1$ ). In all cases the observer is in the direction of the positive  $x$ -axis and the massive star is at  $(0, 0)$ . For a source to be detectable with the current instruments, a lower limit can be set to the energy fluxes:  $F_X > 10^{-14}$  erg/s/cm<sup>2</sup> (*Chandra*, *XMM-Newton*),  $F_{\text{GeV}} > 10^{-11}$  erg/s/cm<sup>2</sup> (*Fermi*) and  $F_{\text{TeV}} > 10^{-13}$  erg/s/cm<sup>2</sup> (*MAGIC*, *HESS*, *VERITAS*). Moreover, in view of the empirical constraints, an upper limit can also be set to the energy fluxes:  $F_X < 10^{-10}$  erg/s/cm<sup>2</sup>,  $F_{\text{GeV}} < 10^{-9}$  erg/s/cm<sup>2</sup> and  $F_{\text{TeV}} < 10^{-11}$  erg/s/cm<sup>2</sup>.

amount of observed strong  $\gamma$ -ray emitters. More specifically:

$$\left( \frac{L_{\text{inj}}}{10^{36}} \frac{\text{erg}}{\text{s}} \right) \left( \frac{d}{3 \text{ kpc}} \right)^{-2} < 0.1 - 1 .$$

However, there could be more sources with such characteristics if they are weaker and/or at a farther distance (so rather sparse), and they would be observable in the GeV and TeV range in the most favourable orbital phases.

- There could be a considerable number of sources that are currently below the sensitivity of the detectors, as galactic sources with intense magnetic fields are weak  $\gamma$ -ray emitters, and so they would be hard to detect in gamma rays at a distance  $> 3$  kpc.

Adiabatic losses are probably important in the farther regions of the system, so we might have overestimated the emission, specially in the X-ray band. In future works we will explore how the introduction of adiabatic losses affects these results, as well as other effects like the radiation from the secondary pairs and the introduction of a hadronic component. We will also use the emissivity maps as a tool for studying properties such as the  $\gamma$ -ray luminosity function of high-mass binaries, their lifespan, etc.

**Acknowledgments.** This work is supported by CONICET and by ANPCyT (PICT 2012-00878). V.B-R. acknowledges financial support from MINECO and European Social Funds through a Ramón y Cajal fellowship. This research has been supported by the Marie Curie Career Integration Grant 321520. V.B-R. and G.E.R. acknowledges support by the Spanish Ministerio de Economía y Competitividad (MINECO) under grant AYA2013-47447-C3-1-P.

## References

- Barret, D. 2004, AIPC, 703, 238  
 Benaglia, P. & Romero, G. E. 2003, A&A, 399, 1221  
 Bosch-Ramon, V., Khangulyan, D. & Aharonian, F. A. 2008, A&A, 482, 397  
 Bosch-Ramon, V. & Khangulyan D. 2009, IJMPD, 18, 347  
 Dubus, G. 2013, A&A Rev., 21, 64  
 Eichler, D. & Usov, V. V. 1993, ApJ, 402, 271.  
 Gould, R. J. & Schröder, G. P. 1967, Phys. Rev., 155, 1408  
 Khangulyan, D., Hnatic, S., Aharonian, F. & Bogovalov, S. 2007, MNRAS, 380, 320  
 Maraschi, L. & Treves, A. 1981, MNRAS, 194, 1  
 Mirabel, I. F. & Rodríguez, L. F. 1994, Nature, 371, 46  
 Mirabel, I. F., & Rodríguez, L. F. 1999, ARA&A, 37, 409  
 Paredes, J. M., Bednarek, W., Bordas, P. et al. 2013, APh., 43, 301